An Electrical Network Approach to the Analysis of Semiconductor Devices

Bogdan M. Wilamowski, *Senior Member, IEEE*, Zbigniew J. Staszak, *Senior Member, IEEE*, and Roy H. Mattson, *Fellow, IEEE*

***Abstract*—A simple electrical network is used to represent the five differential equations describing basic phenomena in one-dimensional semiconductor devices. Both standard and integrated approaches for solving transport equations are developed. Also, an electrical network equivalent for the nonlinear Poisson equation was derived. It allows students to better understand the physical phenomena and the process of computer simulation of such semiconductor devices.**

List of Symbols

A	cross-sectional area, cm^2
C	capacitance, F
D_p and D_n	hole and electron diffusion constants
E	electric field, V/cm
E_{MAX}	maximum electric field
I_p and I_n	the hole and electron currents
J_p and J_n	the hole and electron current densities
k	Boltzman's constant, $1.38 \cdot 10^{-23}$ J/K = $8.62 \cdot 10^{-5}$ eV/K
kT	thermal energy, eV
N_D and N_A	the concentrations of donors and acceptors, respectively
N	the ionized impurity concentration ($N = N_D - N_A$)
n_i	the intrinsic carrier concentration, $1.5 \cdot 10^{10}$ cm^{-3} for Si at 300 K
n_t	the trap concentration at or near the center of the forbidden gap
p and n	densities of holes and electrons
$\overline{p}$ and $\overline{n}$	"average values" of hole and electron concentrations
Q	charge, C
q	the electron charge, $1.6 \cdot 10^{-19}$ C
R	the hole-electron recombination rate, cm^{-3} s^{-1}
T	absolute temperature, K
t	time, s
Δt	time increment, s
V_T	thermal potential, 25.8 mV for $T = 300$ K
x	distance, μm
Δx	length, μm
W	junction depth, μm
μ_p and μ_n	hole and electron mobilities, $cm_2/V \cdot s$
ψ	the electrostatic potential, V
τ_p and τ_n	the hole and electron minority-carrier lifetimes
ε_s	the dielectric constant for semiconductor, 11.8 for Si
ε_0	permittivity of free space, $8.854 \cdot 10^{-14}$ F/cm

Manuscript received February 1990; revised January 1991.

B. M. Wilamowski is with the Department of Electrical Engineering, University of Wyoming, Laramie, WY 82071-3295.

Z. J. Staszak is with the Department of Electronics, Technical University of Gdansk, 80-952 Gdansk, Poland.

R. H. Mattson is with the National Technological University, Fort Collins, CO 80526.

IEEE Log Number 9106738.

I. Introduction

THE learning process for engineering students is often enhanced by the use of models. For example, they learn to understand physics with simple models involving point charges, solid electrons (Bohr model), and analogies to phenomena they already understand.

Electrical engineering students approaching the topics of semiconductor device analysis already have an understanding of electric circuits, but usually lack knowledge about electrical transport phenomena and solid-state physics. Therefore, it is useful to present semiconductor device operation in terms of circuit models. This paper shows that a simple electrical network can be used to model a one-dimensional semiconductor device.

The five differential equations describing basic phenomena in semiconductor devices are relatively difficult for students to comprehend. This paper shows an approach in which a semiconductor device is represented as a simple electrical network depicting these equations in one-dimension. It allows students to better understand the phenomena and the process of computer simulation of semiconductor devices.

Most of the existing computer simulation programs for semiconductor devices use various combinations of simplifying assumptions, e.g., space-charge neutrality, depletion approximation, neglecting recombination, dominance of one type of carriers, neglecting fast transitions that are shorter than relaxation times, etc. However, in many cases such as for small geometry high-speed devices for VLSI applications, these assumptions are not valid and a more general and versatile approach is needed. The program that results from the approach presented here allows for the general analysis of a semiconductor structure without knowledge of any internal conditions. The required input data consists of the impurity concentration distribution as a function of distance and the applied terminal voltages. The simulation includes all effects and provides detailed information about the static and transient

0018-9359/92/0500$03.00 © 1992 IEEE

behavior of semiconductor devices such as the potential, electric field, charge, hole and electron concentrations, hole and electron currents, recombination rate, etc. Only then can the user/student understand what kind of simplifying assumptions can be used and under what conditions.

The paper proceeds as follows. First, a representation of the differential equations by an electrical network will be given followed by a discussion of an improved approach to the differential transport equations. Next, an electrical representation of the nonlinear Poisson equation for the Gummel iterative procedure will be described. The paper includes various examples.

II. Representation of Semiconductor Differential Equations by an Electrical Network

Equations (1)–(6) are basic differential equations describing device behavior for the one-dimensional case as a function of doping concentrations, carrier parameters, and applied voltages.

Transport Equations

$$J_p = -qD_p\frac{dp}{dx} - q\mu_p p\frac{d\psi}{dx} \tag{1}$$

$$J_n = qD_n\frac{dn}{dx} - q\mu_n\frac{d\psi}{dx} \tag{2}$$

where J_p and J_n are the hole and electron current densities, q the electron charge, D_p and D_n hole and electron diffusion constants, p and n densities of holes and electrons, μ_p and μ_n hole and electron mobilities, and ψ is the electrostatic potential.

Continuity Equations

$$\frac{dp}{dt} = -\frac{1}{q}\frac{dJ_p}{dx} - R \tag{3}$$

$$\frac{dn}{dt} = \frac{1}{q}\frac{dJ_n}{dx} - R \tag{4}$$

where t is time, and R is the hole-electron recombination rate given by:

$$R = \frac{np - n_i^2}{\tau_p(n + n_t) + \tau_n(p + n_t)} \tag{5}$$

where n_i is the intrinsic semiconductor carrier concentration, τ_p and τ_n are the hole and electron minority-carrier lifetimes, and n_t is the trap concentration at or near the center of the forbidden gap.

Poisson Equation

$$\frac{d^2\psi}{dx^2} = -\frac{q}{\varepsilon_s\varepsilon_o}(N_D - N_A + p - n) \tag{6}$$

where $\varepsilon_s\varepsilon_o$ is the dielectric constant, and N_D and N_A are the concentrations of donors and acceptors, respectively.

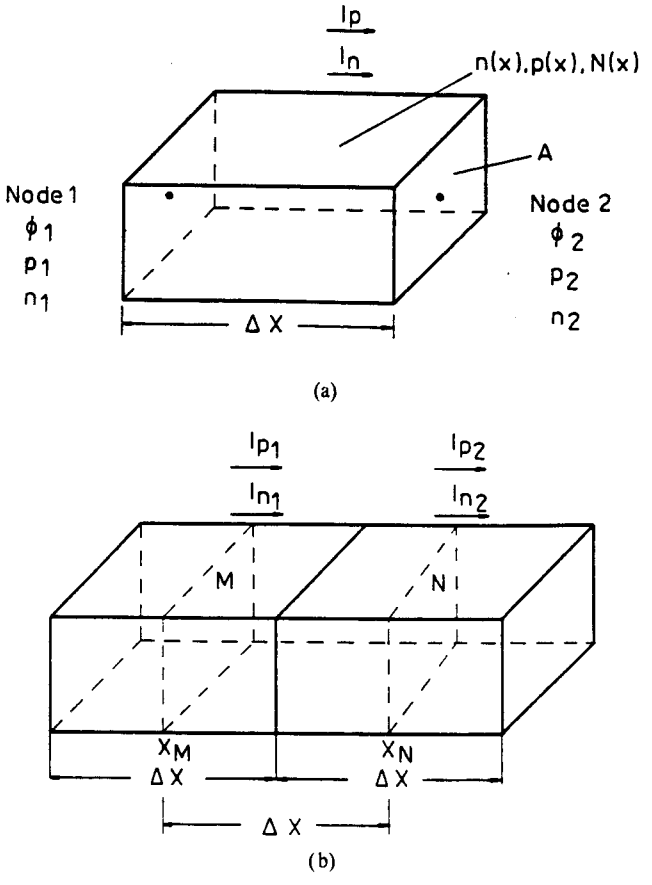

Fig. 1. Physical models of a semiconductor of length Δx and cross-section A. (a) Defining volume between nodes 1 and 2. (b) Defining volume between planes M and N positioned at x_M and x_N, respectively.

The five unknowns are the current densities (J_p, J_n), the carrier concentrations (p, n), and the electrostatic potential (ψ). All are functions of position x and time t as well as doping profiles (determined by fabrication), and the voltages V applied to the device. The quantities D_p, D_n, μ_p, μ_n, R, τ_p, and τ_n need not be constant and could be weak functions of other variables (p, n, N, E). The intrinsic carrier concentration n_i is determined by the temperature and energy gap.

The next step will be to develop an electrical network whose performance accurately predicts the performance of the desired unknowns. This could be done at discrete points in the one-dimensional model of the semiconductor. The discretization is made using the standard finite-difference technique.

A. Transport Equations

Consider a small section of a semiconductor of length Δx and cross-section A as in Fig. 1(a). Modifying (1) and (2), in view of Fig. 1(a), gives:

$$I_p = -AqD_p\frac{p_2 - p_1}{\Delta x} + Aq\mu_p\bar{p}\frac{\psi_1 - \psi_2}{\Delta x} \tag{7}$$

$$I_n = AqD_n\frac{n_2 - n_1}{\Delta x} + Aq\mu_n\bar{n}\frac{\psi_1 - \psi_2}{\Delta x} \tag{8}$$

where I_p and I_n are the hole and electron currents, and $\bar{p}$ and $\bar{n}$ are the "average values" of the hole and electron concentrations. In the simplest case, $\bar{p} = 0.5(p_1 + p_2)$ and $\bar{n} = 0.5(n_1 + n_2)$.

Equations (7) and (8) can be rewritten as:

$$I_p = I_p^* + G_p(\psi_1 - \psi_2) \quad (9)$$

$$I_n = I_n^* + G_n(\psi_1 - \psi_2) \quad (10)$$

giving components of equivalent electrical networks with current sources I_p^* and I_n^* representing diffusion currents, and conductances G_p and G_n simulating the effect of drift. Both currents and conductances are functions of carrier concentrations, and can be given as

$$I_p^* = -AqD_p\frac{p_2 - p_1}{\Delta x} \qquad G_p = Aq\mu_p\frac{p_2 + p_1}{\Delta x} \quad (11)$$

$$I_n^* = AqD_n\frac{n_2 - n_1}{\Delta x} \qquad G_n = Aq\mu_n\frac{n_2 + n_1}{\Delta x} \quad (12)$$

B. Continuity Equations

Equations (3) and (4) can be rearranged based on the physical model of Fig. 1(b). For equal values of Δx, one obtains:

$$\frac{dp}{dt} = -\frac{I_{p2} - I_{p1}}{qA\Delta x} - R \quad (13)$$

$$\frac{dn}{dt} = \frac{I_{n2} - I_{n1}}{qA\Delta x} - R. \quad (14)$$

The region between planes "M" and "N" positioned at x_M and x_N, respectively, is considered a volume (section) ζ. The rectangular solid Δx long with area A can collect mobile carriers. In addition, the solid can be a source of current I_R due to generation-recombination mechanisms. Equations (13) and (14) can then be rewritten as:

$$\frac{dp}{dt} = -\frac{1}{q\zeta}(I_{p2} - I_{p1} - I_R) \quad (15)$$

$$\frac{dn}{dt} = \frac{1}{q\zeta}(I_{n2} - I_{n1} - I_R) \quad (16)$$

where ζ and I_R are given by:

$$\zeta = \Delta x A \quad (17)$$

$$I_R = q\zeta R. \quad (18)$$

It is important to note that (15) and (16) must be used for solving transient or time-varying problems. They show that the rate of change of the carrier concentrations in an infinitesimal volume ($\zeta = \Delta x A$) are linearly related to the sum of the current-generated I_R in the volume ζ, and to the net current entering the volume with appropriate algebraic sign.

C. Poisson Equations

Equation (6) can also be rearranged to provide an equivalent network representation which can be combined with the preceding developments for a complete representation. Integrating (6) for the physical structure of Fig. 1(b) gives:

$$-\frac{d\psi}{dx} = \frac{q\int_{x_M}^{x_N}(p - n + N)\,dx}{\varepsilon_s\varepsilon_o} = \frac{\Delta Q}{\varepsilon_s\varepsilon_o A} \quad (19)$$

where N is the ionized impurity concentration ($N = N_D - N_A$). ΔQ represents the amount of uncompensated or free charge in section MN and is given by:

$$\Delta Q = qA\int_{x_M}^{x_N}(p - n + N)\,dx. \quad (20)$$

For small Δx, (19) can also be written as:

$$-\frac{\Delta Q}{\Delta\psi} = \frac{\varepsilon_s\varepsilon_o A}{\Delta x} = C. \quad (21)$$

Thus, in an electrical analog network representation, the Poisson equation can be represented as a capacitance C (of area A, plate spacing Δx, and dielectric constant $\varepsilon_s\varepsilon_o$) and a "charge source" ΔQ representing the unbalanced charge at the node. Since each infinitesimal section connects between nodes, the capacitance C has to be placed between them. The free charge is unique to each section so it is connected to the common or "ground."

Fig. 2(a) presents the physical structure, and Fig. 2(b) depicts an equivalent electrical network representation which will treat the transport phenomena equations (1), (2) and space charge effects predicted by the Poisson equation (6). The time-varying effects associated with the continuity equations will be included later. These two figures provide physical insight into what is happening in the slice of semiconductor material. The currents I_p^* and I_n^* are diffusion currents caused by carrier concentration gradients, the conductances G_p and G_n are related to the field-induced drift of the carriers, the capacitance C is simply the slice capacitance, and ΔQ is the value of the steady-state free charge stored in that slice. The values of the current generators, conductances, and the stored charge are all functions of carrier concentrations known from the calculations at the previous time step. Such a linear network can be easily solved, e.g., by one of many circuit analysis programs.

To obtain the transient solution, the RC network for a specified time step Δt is transformed into a network containing only resistors and current sources by replacing all capacitances with resistances/conductances and current sources, and fixed charges with current sources. Note the fundamental similarity with switched-capacitor modeling techniques. This rather standard approach is illustrated in Fig. 2(c). This transformed form lends itself to numerical solutions.

To seek a solution of the semiconductor phenomena, based on the equivalent electrical network, conceptually amounts to the following steps if an appropriate computer program is available.

1) Choose values of Δx based on physical understanding; this will determine the number of nodes needed to solve the problem.

2) Choose values of Δt based on physical understanding; this will determine how long the program will have to run.

3) Introduce values for diffusion lifetime, and mobility parameters which can be functions of the unknowns.

4) Introduce initial conditions; usually this consists of applying an external voltage so ψ is fixed at two points, say at $x = 0$ and $x = (m - 1)\Delta x$, where m is the number of nodes.

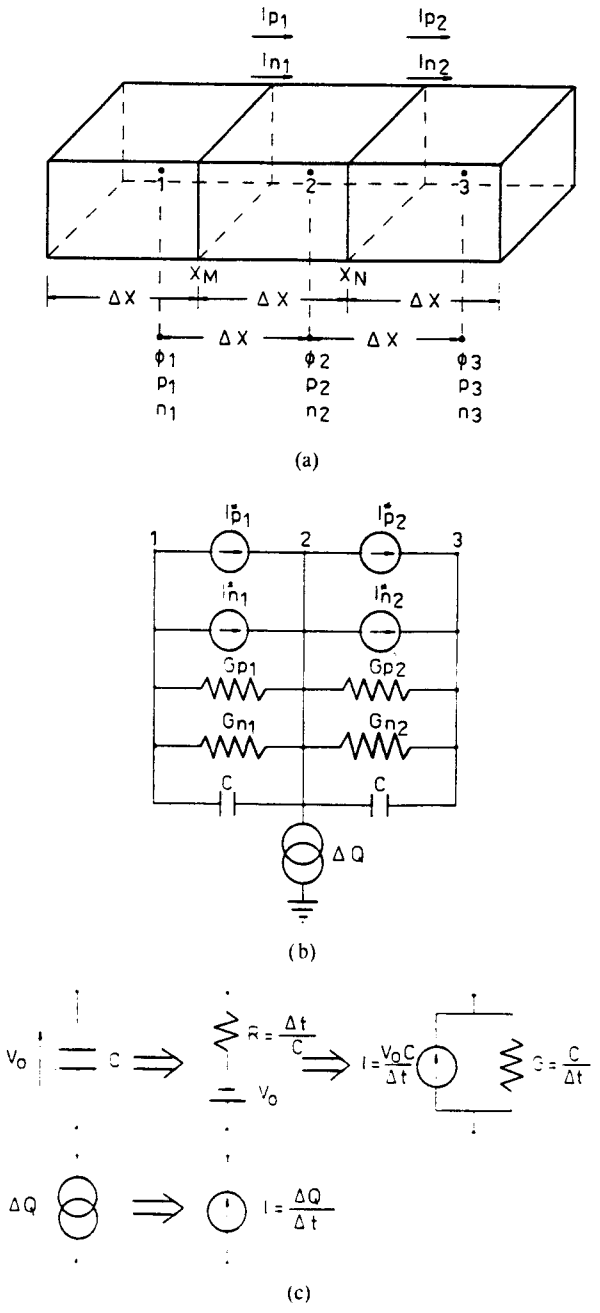

Fig. 2. (a) Physical model of a three-node-semiconductor slab. (b) Equivalent network representation of (1), (2), and (6). (c) Transformation of circuit elements to account for transient phenomena. $I_{p1/2} = -qAD_p\Delta p/\Delta x$, $I_{n1/2} = -qAD_n\Delta n/\Delta x$, $G_{p1/2} = qA\mu_p p/\Delta x$, $G_{n1/2} = qA\mu_n n/\Delta x$, $C = A\varepsilon_s\varepsilon_0/\Delta x$, $\Delta Q = qA(p - n + N)\Delta x$.

It is possible to start with all unknowns equal to zero but intelligent estimates of the carrier concentration values as a function of x and t reduce computer run time. To obtain a steady-state solution, the computer is programmed to repeat runs using the solutions of the preceding run as the initial conditions for the next run. A steady-state solution is assumed complete when there is an acceptably small change in the solutions indicating convergence. In all cases, the results must be evaluated to determine acceptability based on physical insight. During the first run, the computer solves for the node potentials and currents based on the estimated values of carrier concentrations. The resulting hole and electron node currents are unbalanced but known. They can be used in (17) and (18) along with an appropriate generation current to calculate dp/dt and dn/dt at each node. Values for Δp and Δn can be calculated as shown below.

$$\Delta p = -\Delta t\frac{1}{q\zeta}(I_{p2} - I_{p1} - I_R) \tag{22}$$

$$\Delta n = \Delta t\frac{1}{q\zeta}(I_{n2} - I_{n1} - I_R). \tag{23}$$

The new values of carrier concentrations are obtained by correcting the values from the previous time step taking the calculated Δp and Δn from (24) and (25). The carrier concentrations change with time as the slice of material acts as a sink on a source of carriers depending on the effect of external applied voltages. The slice volume ζ acts as the sink or source during an infinitesimal time period Δt. At the end of this time period, the slice volume free charge changes by an amount determined by the change in carrier concentrations at the node. Then, the network parameter values (which are functions of p and n) are calculated, and the computing cycle is repeated.

Key issues include how low the values of p and n should continue to be corrected and what value of Δt should be chosen at each iteration. It is obvious that, for very small changes of n and p per run, convergence can be assured. At the same time, the number of iterations to obtain a steady-state solution can be very large. Based on experience, fast solutions result when the incremental time step is slightly smaller than the time constant τ of each of the calculated nodes.

$$\Delta t < \tau = \frac{\sum C}{\sum G_p + \sum G_n}. \tag{24}$$

The steady-state solution for a reverse biased p–n junction is shown in Fig. 3(a)–3(d) where potential ψ, electric field E, charge Q, hole p, and electron n distributions are shown for various biasing voltages V. When compared with analytical solutions resulting from a depletion approximation, a very good agreement is noted. For example, when plotting the thickness of depletion layers in the p- and n-type regions (W_1 and W_2, respectively) and maximum electric field (E_{max}) as a function of bias voltage (Fig. 4), one can see an excellent correlation of results.

III. Integrated Approach to Transport Equations

It is known that the accuracy of solution for (1)–(4) and (6) is relatively poor when a simple discretization is used. Improved results can be obtained if the integrated form of these differential equations is used. This approach is known as the modified Gummel–Scharfetter method [2], [3]. In this section of the paper, a similar algorithm with the network approach will be presented.

Two adjacent nodes with carrier concentration p_1, n_1 and p_2, n_2 are assumed to have a constant electric field E between them. This field causes a potential difference between the nodes $\Delta\psi = -E\Delta x$, where $\Delta\psi = \psi_2 - \psi_1$ and ψ_1 and ψ_2 represent potentials at these two adjacent nodes. This difference impacts on the carrier concentrations in an

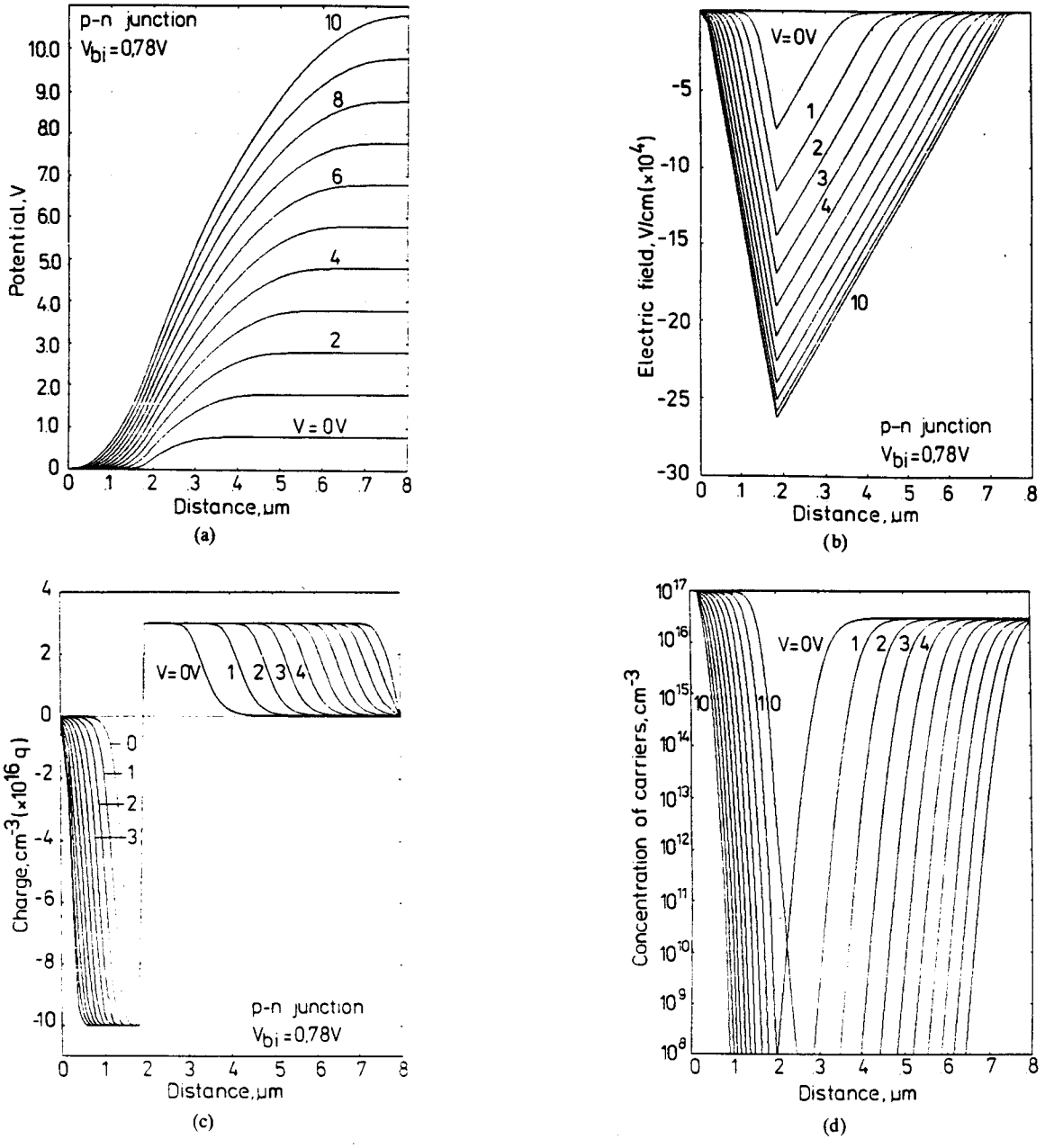

Fig. 3. Steady-state analysis of a reversed-biased p–n junction. (a) Potential v; (b) Electric field E', (c) Q', and (d) holes p and electrons n distributions with bias voltage V as parameter changing from 0 to 10 V; p–n junction parameters: built-in potential $V_{bi} = 0.78$ V, doping concentrations, 10^{17} and $3 \cdot 10^{16}$ cm^{-3}.

exponential manner. It can be shown (see the Appendix) that:

$$J_p = q\mu_p E \frac{p_2 \exp\left(\frac{\Delta v}{2V_T}\right) - p_1 \exp\left(\frac{-\Delta v}{2V_T}\right)}{\exp\left(\frac{\Delta v}{2V_T}\right) - \exp\left(\frac{-\Delta v}{2V_T}\right)} \tag{25}$$

$$J_n = q\mu_n E \frac{n_1 \exp\left(\frac{\Delta \psi}{2V_T}\right) - n_2 \exp\left(\frac{-\Delta \psi}{2V_T}\right)}{\exp\left(\frac{\Delta \psi}{2V_T}\right) - \exp\left(\frac{-\Delta \psi}{2V_T}\right)} \tag{26}$$

where V_T is the thermal voltage ($V_T = kT/q$). k is the Boltzman's constant, T is the absolute temperature, and q is the electron charge.

These equations can also be written in the form of:

$$J_p = q\mu_p E p_{\text{eff}} \tag{27}$$

$$J_n = q\mu_n E n_{\text{eff}} \tag{28}$$

where

$$p_{\text{eff}} = \frac{p_2 \exp(\beta) - p_1 \exp(-\beta)}{\exp(\beta) - \exp(-\beta)} \tag{29}$$

$$n_{\text{eff}} = \frac{n_1 \exp(\beta) - n_2 \exp(-\beta)}{\exp(\beta) - \exp(-\beta)} \tag{30}$$

or

$$p_{\text{eff}} = \frac{p_1 + p_2}{2} + \frac{p_2 - p_1}{2} \frac{1}{\tanh(\beta)} \tag{31}$$

$$n_{\text{eff}} = \frac{n_1 + n_2}{2} - \frac{n_2 - n_1}{2} \frac{1}{\tanh(\beta)} \tag{32}$$

where $\beta = \Delta\psi/2V_T = -E\Delta x/2V_T$.

Equations (27) and (28) can also be rewritten in a form similar to (9) and (10), leading to the same network representation as in Section II. In particular, for small values of

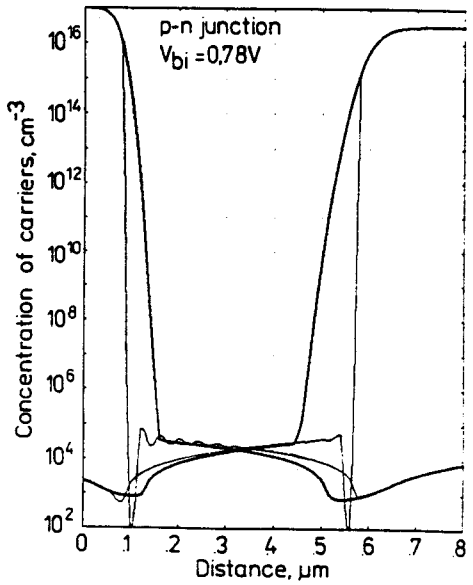

Fig. 4. Comparison of computed and analytically calculated (depletion approximation) parameters. Formulas used in the calculations: $E_{max} = qN_1W_1/\varepsilon_s\varepsilon_o = qN_2W_2/\varepsilon_s\varepsilon_o$, $W_1 = (2\varepsilon_s\varepsilon_o/qN_1(1 + N_1/N_2))^{0.5}$, $W_2 = (2\varepsilon_s\varepsilon_o/qN_2(1 + N_2/N_1))^{0.5}$, with $N_1 = 10^{17}$ cm^{-3} and $N_2 = 3 * 10^{16}$ cm^{-3}. Numerical values for W_1 and W_2 were obtained from the plot of electric field versus distance by intersecting extensions of the respective electric field plots with the horizontal (distance) axis.

β ($\tanh(\beta) \approx \beta$), (27) and (28) take the forms of (11) and (12).

To discuss (25) and (26), let us consider three simplified cases.

a) Case 1: For $p_{\text{eff}} = p_1 = p_2 = p$ and $n_{\text{eff}} = n_1 = n_2 = n$ when only drift currents exist. Equations (25) and (26) reduce to:

$$J_p = q\mu_p pE \tag{33}$$

$$J_n = q\mu_n nE \tag{34}$$

b) Case 2: When diffusion is the dominant mechanism, $|E| \ll V_T/\Delta x$. Then (25) and (26) will simplify to:

$$J_p = -qD_p\frac{p_2 - p_1}{\Delta x} \tag{35}$$

$$J_n = qD_n\frac{n_2 - n_1}{\Delta x} \tag{36}$$

which are the typical diffusion equations.

c) Case 3: When the electrical field is high and drift is a dominant mechanism, $|E| \gg V_T/\Delta x$. Then the results depend on the direction of electrical field.

If $\Delta\psi$ is positive:

$$J_p = q\mu_p p_2 E \tag{37}$$

$$J_n = q\mu_n n_1 E. \tag{38}$$

If $\Delta\psi$ is negative:

$$J_p = q\mu_p p_1 E \tag{39}$$

$$J_n = q\mu_n n_2 E. \tag{40}$$

It should be stressed that the current calculations depend on the direction is which the carriers are moving. The concentration of either the left or right node is used, depending on the carrier and field direction to calculate current. This approach is known as the "down wind–up wind" approach of solution of partial differential equations.

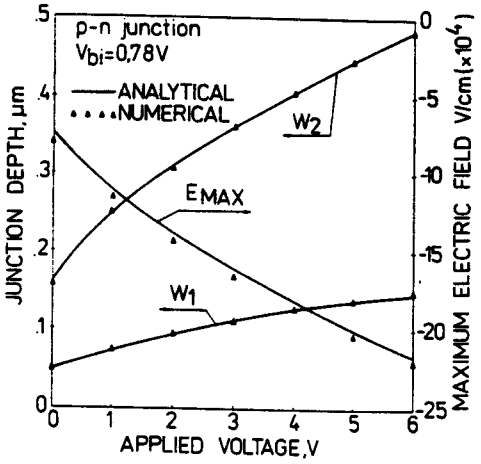

Fig. 5. Comparison of results of hole and electron current distribution of a reversed- biased $p-n$ junction at steady-state: integrated approach (thick lines) and of the standard finite-difference approach as described in Section II (thin lines) with 41 mesh points as compared to 161 points as for examples shown in Section II; a bias voltage of 5 V has been used.

For moderate electrical fields, the effective values of the carrier concentrations are calculated from (31) and (32). Using the integrated form to calculate the currents, better accuracy can be obtained. At the same time, the section size could be bigger and thus the number of discrete points smaller.

A reverse biased $p-n$ junction has been analyzed using this approach. Example results of steady-state hole and electron currents distributions are presented in Fig. 5. Using the integrated approach (thick lines), four times fewer mesh points (41 points) have been used to obtain similar results as compared to the simplified (standard finite-difference) approach described in Section II (thin lines) where 161 points had to be used. It can be seen that the simplified approach introduces significant errors, while the integrated approach gives correct results even for the range of changes of 15 orders of magnitude.

IV. Method of Solution for Poisson Equation

In order to be able to use the most common Gummel iterative procedure [1]–[3], the Poisson equation has to be written in a nonlinear form

$$\frac{d^2\psi}{dx^2} = -\frac{q}{\varepsilon_s\varepsilon_o}(p - n + N) \tag{41}$$

with

$$\psi = \psi_o + \delta\psi \tag{42}$$

$$p = p_o \exp\left(\frac{-\delta\psi}{V_T}\right) \tag{43}$$

$$n = n_o \exp\left(\frac{\delta\psi}{V_T}\right) \tag{44}$$

where $\delta\psi$ is the voltage increment from one iteration to the other, and ψ_o, p_o, and n_o are the values from the previous iterations.

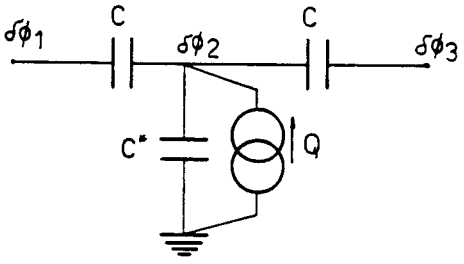

Fig. 6. Network representation of (49).

After inserting (42)–(44) into (41), one obtains:

$$\frac{d^2\psi_o}{dx^2} + \frac{d^2(\delta v)}{dx^2} = \frac{q}{\varepsilon_s\varepsilon_o}(n_o - p_o - N) + \frac{q}{\varepsilon_s\varepsilon_o}(n_o + p_o)\frac{\delta v}{V_T} \tag{45}$$

where, in the discretized case (uniform mesh),

$$\frac{d^2(v_o)}{dx^2} = \frac{v_{o1} + v_{o3} - 2v_{o2}}{\Delta x^2} \tag{46}$$

$$\frac{d^2(\delta v)}{dx^2} = \frac{\delta v_1 + \delta v_3 - 2\delta v_2}{\Delta x^2}. \tag{47}$$

Substituting $\delta\psi = \delta v_2$, insetting (46) and (47) into (43), and multiplying it by $-\Delta x A\varepsilon_s\varepsilon_o$, one obtains:

$$-\frac{A\varepsilon_s\varepsilon_o}{\Delta x}\delta v_1 + \left[\frac{2A\varepsilon_s\varepsilon_o}{\Delta x} - \frac{A\Delta x q(n_o + p_o)}{V_T}\right] \cdot \delta v_2 - \frac{A\varepsilon_s\varepsilon_o}{\Delta x}\delta v_3 = A\Delta x q(n_o - p_o - N) - \frac{A\varepsilon_s\varepsilon_o}{\Delta x}(v_{o1} + v_{o3} - 2v_{o2}) \tag{48}$$

or

$$-C\delta\psi_1 + (2C - C^*)\delta\psi_2 - C\delta v_3 = Q \tag{49}$$

where

$$C = \frac{A\varepsilon_s\varepsilon_o}{\Delta x} \tag{50}$$

$$C^* = \frac{A\Delta x q(n_o + p_o)}{V_T} \tag{51}$$

$$Q = A\Delta x q(n_o - p_o - N) - \frac{A\varepsilon_s\varepsilon_o}{\Delta x} \cdot (v_{o1} + v_{o3} - 2\psi_{o2}). \tag{52}$$

Equation (49) corresponds to the network shown in Fig. 6. One can notice that the nonlinear approach (Gummel method) results in large grounded capacitances. This makes the network matrix principal diagonal significantly dominant, and a simple iterative procedure can be used for solution.

V. Examples

Various semiconductor devices were analyzed. Fast results are possible for one-dimensional analysis and this allows students to understand the principles of operation of such specialized semiconductor devices as Camel, Gunn, and TRAPATT diodes to name only a few. For example, Figs. 7 and 8 [4] present results for a device which operates in a punch-through condition with space-charge control of currents. The structure of the device is simple with two n^+ or p^+ regions formed in p^- or n^- substrate, respectively. Fig. 7(a)–(d) shows the results of a steady-state analysis for an $n^+p^-n^+$ structure after punch-through with bias voltage changing from -0.5 to 5 V. Fig. 8(a) and (b) presents the results of a transient analysis for a $p^+n^-p^+$ structure during switching from 2 to 10 V as a function of time in 30 ps increments. Observe the mechanism of carrier injection over the potential barrier, space-charge limited flow control, and very fast transients.

Other effects can be easily implemented into the program (for example, carrier mobility as function of electrical field, carrier generation electrical field dependence, carrier generation by light, other recombination mechanisms, carrier scattering on impurities and lattice, etc.). All phenomena can also be temperature-dependent.

VI. Conclusion

An electrical network approach for an analysis of the behavior of semiconductor devices has been developed and demonstrated by a number of physical examples. Computer programs exist which may be employed by students to investigate the transient and steady-state behavior of such devices based on the model developed. The models are sufficiently simple as to be run on personal computers.

The usefulness of the approach that has been presented includes:

1) aiding students to understand device phenomena based on models they know how to manipulate,

2) aiding students to understand how a computer device simulator program is developed, and

3) providing students and others with a useful device simulator program that will simulate device performance in the steady-state or transient mode without simplifying assumptions or approximations. It is limited to one dimension, but is considered instructive and useful for educational purposes as well as solving real simple-geometry structures.

The algorithm is very simple and the programs developed were implemented in FORTRAN on a VAX 11/780 minicomputer and in Turbo-Pascal on IBM PC and compatibles. In order to introduce various options in running the programs, elemental knowledge of one of these programming languages is required. Since the programs have built-in plotting capabilities, visualization of processes and dynamic changes of transients occurring in a semiconductor device under various excitation conditions is easy to obtain. Examples of such cases can include, e.g., observation of changes in the distribution of concentration of carriers injected to the base during the bipolar transistor turnoff; distribution of minority carrier concentration in the base-collector region of the bipolar transistor leaving saturation: building up the domain in the Gunn diode; or analyses of various analysis of different reaction times in a photodiode when radiation is absorbed in the depletion region or in the neutral regions near junction, to name only a few. This has a very significant

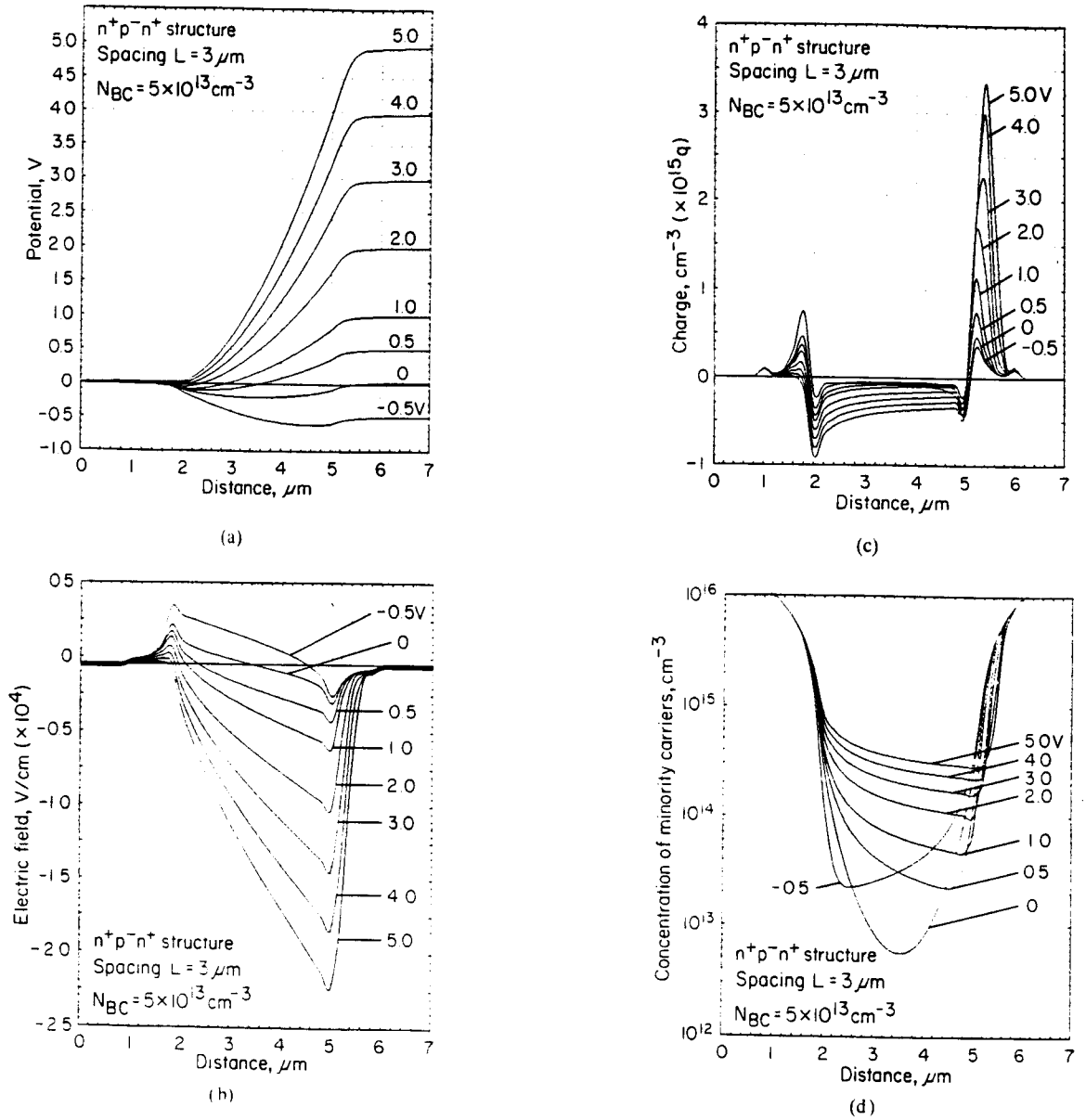

Fig. 7. Steady-state analysis of $n^+p^-n^+$ punch-through structure with spacing between n^+-regions $L = 3$ μm and background concentration of $N_{BC} = 5 \cdot 10^{13}$ cm^{-3}: (a) potential distribution, (b) electric field distribution, (c) space-charge distribution, and (d) minority carriers distribution.

didactic effect in that visualization of phenomena are more easily comprehended by students than written formulas on the blackboard.

Appendix
Derivation of (25) and (26)

Starting with (1),

$$J_p = -qD_p\frac{dp}{dx} - q\mu_p p\frac{dv}{dx} \tag{A1}$$

multiplying by $\exp(v/V_T)$

$$J_p\exp\left(\frac{v}{V_T}\right) = -qD_p\frac{dp}{dx}\exp\left(\frac{v}{V_T}\right) - q\mu_p\frac{dv}{dx}p\exp\left(\frac{v}{V_T}\right) \tag{A2}$$

rearranging

$$J_p\exp\left(\frac{v}{V_T}\right) = -q\mu_p V_T\frac{d}{dx}\left[p\exp\left(\frac{v}{V_T}\right)\right] \tag{A3}$$

performing integration

$$-\int_{x_1}^{x_2}\frac{J_p}{\mu_p q V_T}\exp\left(\frac{\psi}{V_T}\right)dx = \left[p\exp\left(\frac{v}{V_T}\right)\right]\Bigg|_{x_1}^{x_2} \tag{A4}$$

substituting $v = -Ex$

$$\left[\frac{J_p}{\mu_p q V_T}\frac{V_T}{E}\exp\left(\frac{E_x}{V_T}\right)\right]\Bigg|_{x_1}^{x_2} = \left[p\exp\left(\frac{-Ex}{V_T}\right)\right]\Bigg|_{x_1}^{x_2} \tag{A5}$$

and, after some arrangements, one obtains

$$J_p = q\mu_p E\frac{p_2\exp\left(\frac{v_2}{V_T}\right) - p_1\exp\left(\frac{v_1}{V_T}\right)}{\exp\left(\frac{v_2}{V_T}\right) - \exp\left(\frac{v_1}{V_T}\right)}. \tag{A6}$$

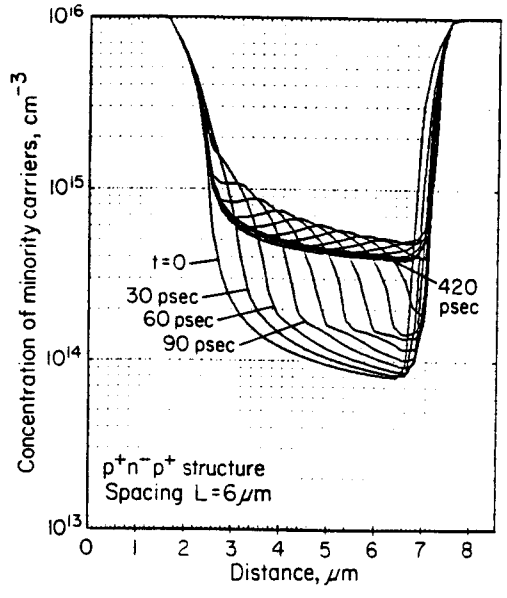

(a)

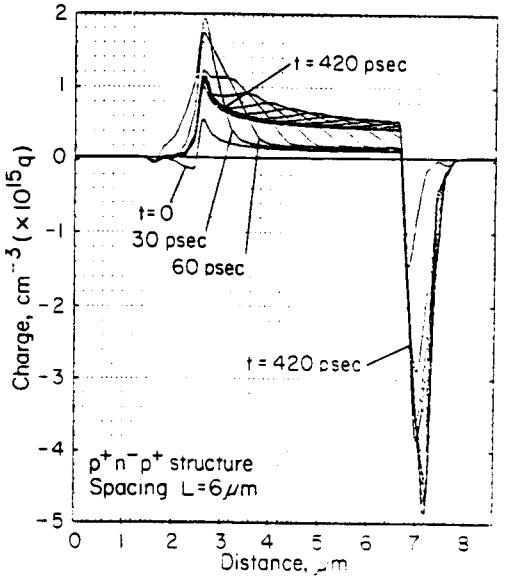

(b)

Fig. 8. Transient analysis of $p^+n^-p^+$ punch-through structure with a spacing between p^+-regions $L = 6$ μm: (a) minority carriers distribution, and (b) space-charge distribution.

After substitution $v_2 = v - \Delta v/2$ and $v_1 = v - \Delta v/2$, the final formula (25) is as follows:

$$J_p = q\mu_p E \frac{p_2 \exp\left(\frac{\Delta v}{2V_T}\right) - p_1 \exp\left(\frac{-\Delta v}{2V_T}\right)}{\exp\left(\frac{\Delta v}{2V_T}\right) - \exp\left(\frac{-\Delta v}{2V_T}\right)}. \qquad \text{(A7)}$$

In a similar way, (26) can be obtained.

REFERENCES

[1] S. Selberherr. *Analysis and Simulation of Semiconductor Devices.* New York: Springer-Verlag, 1984.

[2] H. K. Gummel, "A self-consistent iterative scheme for one-dimensional steady-state transistor calculations," *IEEE Trans. Electron Dev.*, vol. ED-11, pp. 455–465, 1964.

[3] D. L. Scharfetter and H. K. Gummel, "Large signal analysis of a silicon read diode oscillator," *IEEE Trans. Electron Dev.*, vol. ED-16, pp. 63–77, 1969.

[4] B. M. Wilamowski, R. H. Mattson, Z. J. Staszak, and A. Musallam, "Punch-through space-charge limited loads," in *Proc. 36th Electron. Compon. Conf.*, Seattle, WA, May 1986, pp. 399–404.

Bogdan M. Wilamowski received the M.S. degree in computer engineering, the Ph.D. degree in neural computing, and the D.Sc. degree in integrated circuit design from the Technical University of Gdansk, Gdansk, Poland, in 1966, 1970, and 1977, respectively.

He has been with this University since 1966. He became Associate Professor in 1978 and Professor in 1987. During 1979–1981, he was the Director of the Institute of Electronic Technology and, during 1988–1989, he was the Head of the Solid-State Electronic Chair at this University. From 1968 to 1970, he was with the Nishizawa Laboratory at Tohoku University, Japan. In 1975–1976, he spent one year at the Semiconductor Research Institute, Sendai, Japan as a JSPS Fellow. During 1981–1982, he was a faculty member at Auburn University. During 1982–1984, he was a Visiting Professor at the University of Arizona, Tucson. Since 1989, he has been a Professor in the Electrical Engineering Department of the University of Wyoming. He is the author of two books, more than 100 technical publications, and about 30 patents in seven countries. His main areas of interest are semiconductor devices, electronic and integrated circuits, and computer simulation and modeling.

Zbigniew J. Staszak received the M.S. degree in electrical engineering and the Ph.D. degree in the thermal analysis of electronic circuits from the Technical University of Gdansk, Gdansk, Poland, in 1969 and 1978, respectively.

He has been with this University since 1969. He received the Price of Ministry of Education for his outstanding Ph.D. dissertation. He was recognized by the University President as outstanding teacher and researcher. From 1975 to 1976, he was a Visiting Fulbright Scholar at the University of Michigan, Ann Arbor. From 1982 to 1986, he was Visiting Scholar at the University of Arizona, Tucson, where he worked in the area of electronic packing. He is the author of more than 40 technical publications. His main areas of interest are thermal effects, electronic and integrated circuits, and computer simulation and modeling.

Roy H. Mattson was born in Chisholm, MN, on December 28, 1927. After service in the U.S. Navy as an electronic technician, he received the B.S. degree in electrical engineering and the M.S.E.E. degree from the University of Minnesota in 1951 and 1952, respectively, and the Ph.D. degree from Iowa State University, Ames, in 1959.

From 1952 to 1956, he was with Bell Telephone Laboratories. From 1956 to 1961, he was Assistant and then Associate Professor in Electrical Engineering at Iowa State University. He then joined the University of Minnesota as Associate Professor. In 1966, he accepted a position as Professor and Head of Electrical Engineering at the University of Arizona, Tucson. He was Department Head until 1986, and continued as a Professor until 1988. He then joined the National Technological University as Academic Vice President. He has been active in engineering education activities, serving as the Editor for the IEEE TRANSACTIONS ON EDUCATION, the General Chairman of *Frontiers in Education* conference, Chairman of the Electrical Engineering Division for the American Society for Engineering Education, and Chairman of the IEEE Validation of Education Achievement. He has served on the IEEE Education Activities Board and was Chairman of the Electrical Engineering Department Heads Association. He has authored two books, been granted six patents, and published numerous articles.